

# **Enabling Electrical Biomolecular Detection in High Ionic Concentrations and Enhancement of Detection Limit Thereof by Coupling Nanofluidic Crystal with Reconfigurable Ion Concentration Polarization**

Wei Ouyang,<sup>1, 2</sup> Jongyoon Han,<sup>1, 3, \*</sup> and Wei Wang<sup>2, 4, \*</sup>

<sup>1</sup>*Department of Electrical Engineering and Computer Science, Massachusetts Institute of Technology, Cambridge, Massachusetts, 02139, United States*

<sup>2</sup>*Institute of Microelectronics, Peking University, Beijing, 100871, P.R. China*

<sup>3</sup>*Department of Biological Engineering, Massachusetts Institute of Technology, Cambridge, Massachusetts, 02139, United States*

<sup>4</sup>*National Key Laboratory of Science and Technology on Micro/Nano Fabrication, Beijing, 100871, P.R. China*

*\*Correspondence: J. Han, jyhan@mit.edu; W. Wang, w.wang@pku.edu.cn*

## **Supplementary Information**

### S1. Photos of the device

Fig. S1.1(a) shows the backside of the device where the micro-structures on the silicon and glass can be observed. Connections to electrical equipment were also shown. Depending on the experiment design, syringe pumps may or may not be used, as specified in the main text. Fig. S1.1(b) shows the device mounted on a fluorescence microscope. The PDMS slab bonded to the chip and reservoirs made by pipet tips can be observed.

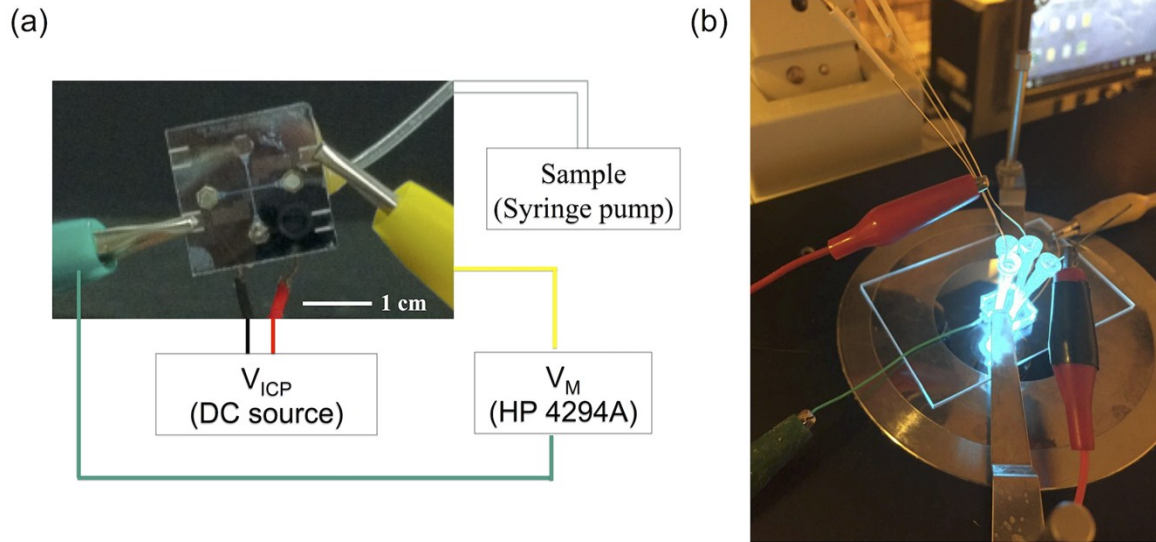


**Fig. S1.1.** (a) Photo of the backside of the device showing micro-structures. (b) Photo of the device mounted on a fluorescence microscope.

## S2. Numerical simulation of the back-diffusion of ions

We simulated the back-diffusion of ions after turning off the voltage for depletion using the Transport of Diluted Species and Laminar Flow modules of COMSOL Multiphysics. The diffusivity of ions is  $1.33 \times 10^{-9} \text{ m}^2/\text{s}$ . The two-dimensional model is shown in Fig. S1. Four orthogonal microchannels are 5 mm long and connected, neglecting the nanoparticle crystal and nanofilters. The concentration of the four reservoirs is set to 160 mM ( $1 \times \text{PBS}$ ). The initial conditions are as follows: the depletion zones are  $L$  long ( $L=500, 1000, \text{ and } 1500 \text{ }\mu\text{m}$ ) with a concentration of 0.16 mM (1000-fold depletion); outside the depletion zones, the initial concentration is 160 mM. In fact, the initial and boundary conditions of the nafion channel cannot be precisely determined, because the concentration of the reservoir of the nafion channel is elevated due to the ICP effect. However, due to the long distance of the reservoir from the nanoparticle crystal, we can simplify the model by neglecting the back-diffusion from the nafion channel and solely focusing on the other three microchannels. We also studied the effect of inter-channel fluid flows on the back-diffusion of ions, which can be caused by the uneven liquid level of the reservoirs. The fluid flow can accelerate the movement of ions towards the nanoparticle crystal, resulting in shortened detection time window. We simulated an in-going flow through the upper central channel with a velocity of  $v$  ( $v=20 \text{ and } 40 \text{ }\mu\text{m/s}$ ), which splits to the two side channels. The flow in the nafion channel is zero, because the nafion channel is mechanically blocked in the depletion mode.

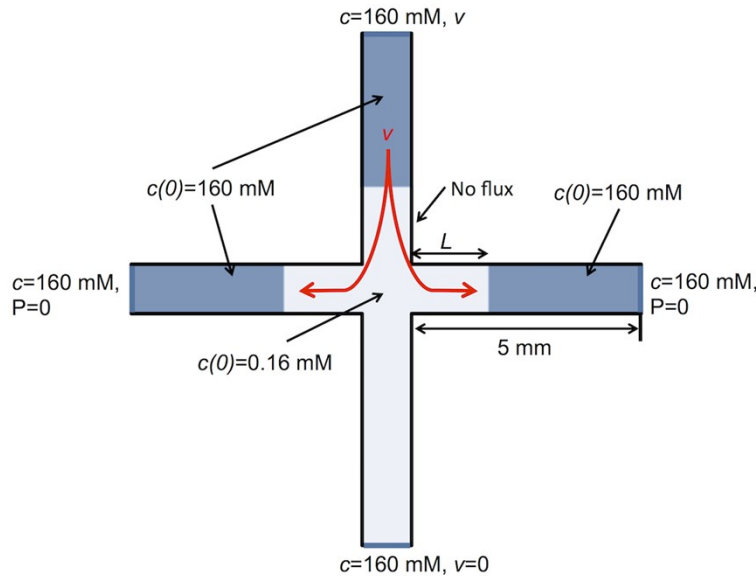


**Fig. S2.1.** Initial and boundary conditions of the COMSOL model.

## S3. Theoretical model of biosensing in nanoparticle crystal

We consider nanoparticles with a diameter of  $D$  packed in a volume of  $W \times L \times H$ . The nanoparticles are packed in a face-center cubic structure, so the space occupation ratio of the

nanoparticles is 74.05%. The volume of a single nanoparticle is  $V_p = \frac{\pi D^3}{6}$ , and the surface area of a single nanoparticle is  $S_p = \pi D^2$ . Therefore, the total number of nanoparticles in the NFC is  $N_p = \frac{0.74WLH}{V_p} = \frac{4.44WLH}{\pi D^3}$ , and the total surface area is  $S_{tot} = S_p \times N_p = \frac{4.44WLH}{D}$ .

The electrical resistance of the NFC is  $R = \frac{0.7405\pi}{2 \times 0.9068^2} \cdot \frac{L}{WH} \cdot D \cdot R_{unit}$ , where  $R_{unit}$  is the electrical resistance of the equivalent unit nanochannel in the NFC, with a diameter of  $D_{unit} = 0.24D$ , and a length of  $L_{unit} = 0.5215D$ . In the surface charge-governed regime, the electrical resistance of the unit nanochannel is determined by the surface charge density, which is

$$R_{unit} = -\frac{1}{\mu_+ \sigma \frac{P}{L}} = -0.692 \frac{1}{\mu_+ \sigma} \quad (P: \text{perimeter of the channel}, \sigma: \text{negative surface charge density}).$$

Therefore, the electrical resistance of the NFC in the surface charge-governed regime is

$$R = -0.978 \frac{L}{WH \mu_+ \sigma} \frac{D}{D}.$$

Let  $z_{probe}$  and  $n_{probe}$  be the charge number and the area density of the sensing probe on the nanoparticle. Let  $z_{SA}$  and  $n_{SA}$  be the charge number and the area density of the surface-coated streptavidin. Then the surface charge density of the nanoparticle before target molecule binding is  $\sigma = z_{probe} e n_{probe} N_A + z_{SA} e n_{SA} N_A = z_{probe} F n_{probe} + z_{SA} F n_{SA}$ , where  $e$ ,  $N_A$ , and  $F$  are the elementary charge, Avogadro number and the Faraday constant.

Let  $V_{sample}$ ,  $c_{tgt}$ ,  $z_{tgt}$ , and  $\eta_{capture}$  be the volume of the sample, the concentration of the target biomolecule in the sample, the charge number of the target biomolecule, and the capturing efficiency of the target biomolecule. The total moles of captured target biomolecules is  $N_{capt\_tgt} = \eta_{capture} V_{sample} c_{tgt}$ . Averaged density of the captured target biomolecules is

$$n_{tgt} = \frac{N_{capt\_tgt}}{S_{tot}} = \frac{\eta_{capture} V_{sample} c_{target}}{\frac{4.44WLH}{D}}. \quad \text{Therefore, the surface charge density of the}$$

nanoparticle after target molecule binding is

$$\sigma' = z_{probe}Fn_{probe} + z_{SA}Fn_{SA} + z_{tgt}Fn_{tgt} = z_{probe}Fn_{probe} + z_{SA}Fn_{SA} + z_{tgt}F \frac{\eta_{capture}V_{sample}}{4.44W}$$

Let  $\alpha$  be the occupation rate of the affinity probes onto the streptavidin binding sites ( $n_{probe} = \alpha n_{SA}$ ). Because that the affinity probes with large molecular weights (MWs) can hide other biotin binding sites on streptavidin,  $\alpha$  is typically less than 100%, and can be reasonably assumed to be proportional to 1/MW of the affinity probe.

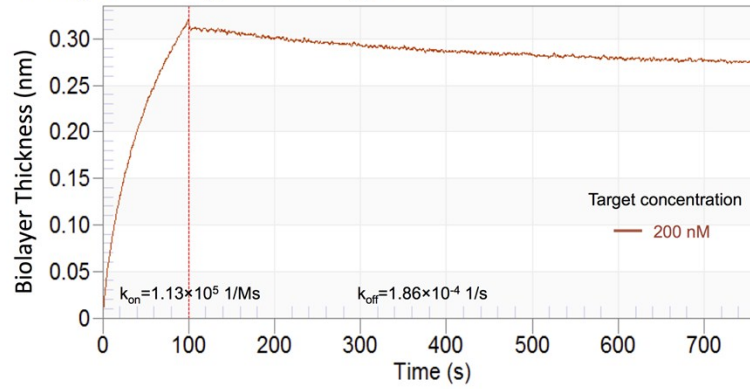
The ratio of the electrical resistance after and before target binding is,

$$\frac{R'}{R} = \frac{\sigma'}{\sigma} = \frac{1}{1 + 0.225 \frac{z_{tgt}}{\alpha z_{probe} + z_{SA}} \cdot \frac{D}{n_{SA}} \cdot \frac{1}{WLH} \cdot \eta_{capture} V_{sample} c_{tgt}}$$

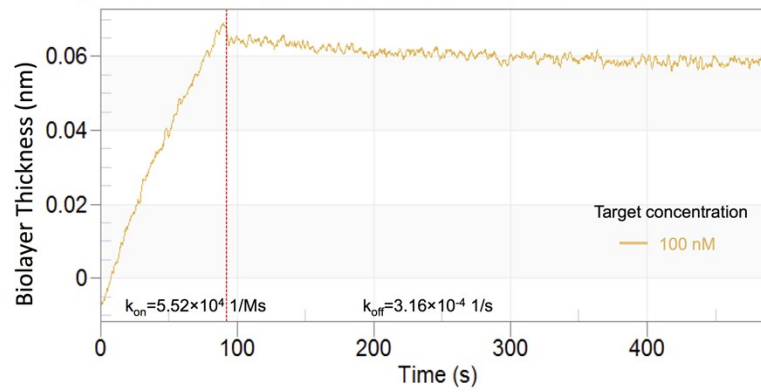
#### S4. Binding kinetics of probe-target biomolecule pairs

The binding kinetics of gp120 Ab-Ag, MTB probe-DNA, and thrombin binding aptamer-thrombin was measured by Octet RED 96. The buffer used was 1xPBS with 1% BSA. First, streptavidin sensor tips were dipped into 20 ug/ml biotinylated gp120 Ab, MTB probe DNA, and thrombin binding aptamer for ligand immobilization, respectively. Next, the association step was conducted, with loaded sensor tips dipped into series concentrations of gp120 Ag, MTB DNA, and thrombin, respectively. Finally, the dissociation step was conducted by dipping the sensor tips into the buffer. The time of each step in measuring different probe-target pairs varied, depending on the association and dissociation rates. The sensorgrams of the binding kinetics are show in Fig. S2.

(a) Binding kinetics of gp120 Ab and gp120 Ag



(b) Binding kinetics of MTB probe DNA and MTB target DNA



(c) Binding kinetics of thrombin binding aptamer and human thrombin

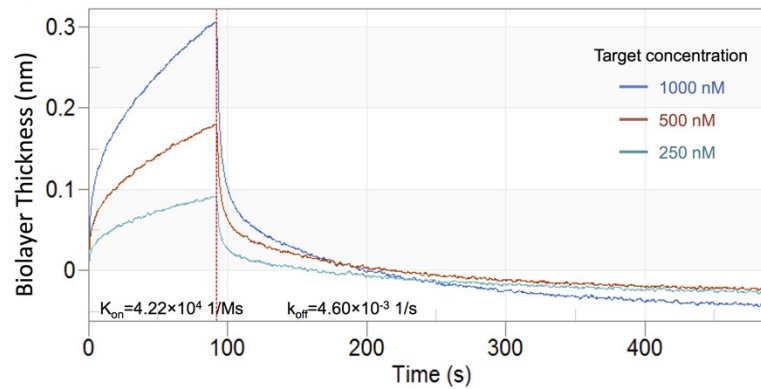


**Fig. S4.1.** Sensorgrams of the binding kinetics of (a) gp120 Ab-gp120 Ag, (b) MTB probe-target DNAs, and (c) thrombin binding aptamer and human thrombin.